Spectral line parameters of hot transitions forming the 6.3-μm band of water vapor

O.N. Sulakshina, Yu.G. Borkov, and R.O. Manuilova[1]

Institute of Atmospheric Optics,
Siberian Branch of the Russian Academy of Sciences, Tomsk
[1] Scientific & Research Institute of Physics at the St. Petersburg State University, St. Petersburg

Received March 13, 2001

Intensities of water vapor absorption lines of the hot bands in the region from 1500 to 2100 cm^{-1} are estimated to update the spectral information needed when studying the kinetics of water vapor vibrational states in the middle atmosphere and non-equilibrium atmospheric emissions. Hot lines in this spectral region are due to transitions from the first triad of vibrational states to the second triad of the excited vibrational states (110, 011, 030). Computation of the line centers is based on the method of effective Hamiltonian and *G*-functions method. The parameters of the effective dipole moment are estimated based on the derivatives of H_2O dipole moment function we have constructed.

Introduction

To study the kinetics of vibrational states of the water molecule in the middle atmosphere and non-equilibrium atmospheric emissions in the IR rovibrational bands from 1.4 to 6.3 μm is an urgent problem in connection with the development of new methods for remote sensing of water vapor in the stratosphere and mesosphere that would account for violation of the local thermodynamic equilibrium (LTE). The importance of the exact knowledge of the water vapor content in the upper stratosphere and mesosphere is motivated by the fact that due to dissociation the concentration of water vapor is closely related with the content of hydrogen- and oxygen-containing atmospheric constituents (H, OH, O, O_3, etc.) at these altitudes. The need in monitoring water vapor content in the mesosphere became even more urgent in connection with the problems of long-term temperature trends (up to 30 K for 40 years at the altitude of 87 km), composition and glow of the middle atmosphere.[1–2] In particular, the drastic decrease in the ozone content predicted based on the 40-year trends in the vicinity of the mesopause is still to be explained.

Recently, the atmospheric emission spectra in the region of water vapor IR bands have been recorded not only using broadband satellite measurements (ISAMS/UARS),[3] but also in the experiments with medium resolution (1 cm^{-1}) (CIRRIS-1A).[4] High-resolution experiments (MIPAS-ENVISAT-1)[5] are planned as well.

In connection with the need to interpret the measurements, especially, those with high resolution, it is necessary to increase the number of excited states and, correspondingly, rovibrational transitions to be included into the model of vibrational kinetics of the H_2O molecule.

According to our estimates, 13 states are to be taken into account, from the first excited state with the quantum number 010 and the energy of 1595 cm^{-1} and up to the 002 state with the energy of 7445 cm^{-1}, as well as 33 vibrational transitions, in contrast to the previous studies,[6,7] which took into account no more than 6 states and 10 transitions. The latest database of spectroscopic parameters of atmospheric gases – HITRAN – does not include all the needed information and has some errors in calculated intensities of hot bands. In Refs. 8 and 9, vibrational states of the water molecule were calculated up to the energy of 28000 cm^{-1}, and transition intensities were estimated from the information on the dipole moment function obtained from *ab initio* calculations. Although quantum chemical calculations give the qualitatively correct description, they do not provide sufficient accuracy for reconstructing the experimental parameters characterizing transitions to highly excited states.

In this paper, we present calculated spectral line parameters for the hot transitions forming the 6.3 μm band, namely, the transitions from the first triad of the excited states (020, 100, 001) to the second triad of the excited states (030, 110, 011). The diagram of energy levels is shown in Fig. 1. In the calculation, we used known methods of effective Hamiltonian and dipole moment[10–13] operators, which worked quite effectively in processing the polyads of interacting states, since they possess the best extrapolation properties. The parameters of the effective dipole moment were estimated based on the derivatives of the dipole moment function of the water molecule we have described in Refs. 14 and 15. The calculated parameters were compared with the literature data (see, for example, Ref. 9). It is an advantage of this method that there is no need in using supercomputers for calculations by this method.

0235-6880/01/12 1016-06 $02.00

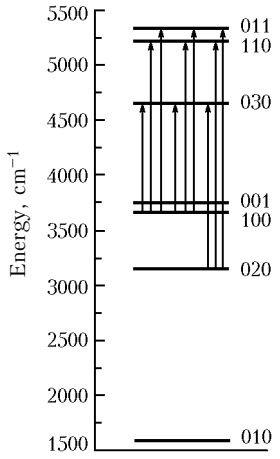

Fig. 1. Diagram of vibrational energy levels of the water molecule in the region from 1500 to 5500 cm^{-1}.

Theoretical models

Effective Hamiltonian

When calculating rovibrational energy levels of the first and second triads, the effective rotational Hamiltonian was constructed for the group of resonant states $\tilde{H}_{\text{eff}}$ accounting for all the resonance interactions among these states:

$$\tilde{H}_{\text{eff}} = \tilde{H}_{\text{diag}} + \tilde{H}_{\text{int}}, \qquad (1)$$

where the operator $\tilde{H}_{\text{diag}}$ is the diagonal part, i.e., the effective Hamiltonian for each of the interacting states, and the operator $\tilde{H}_{\text{int}}$ describes resonance interactions of the Fermi and Coriolis types. As known, various models of the effective rotational operators are used to study the rotational structure of the energy spectrum of the water molecule.[16] In this paper, we selected the method of *G*-functions,[17–19] which made a good showing in description of anomalous centrifugal effects. For each state, the effective rotational Hamiltonian $\tilde{H}_{\text{diag}}$ was written as a sum of the diagonal and off-diagonal operators with respect to the wave functions[16]:

$$\tilde{H}_{\text{diag}} = {}^{\text{d}}H_{\text{rot}} + {}^{\text{n.d}}H_{\text{rot}}, \qquad (2)$$

where

$$ {}^{\text{d}}H_{\text{rot}} = \sum_m g_m^{(J)} \{\mathbf{G}(\alpha^{(J)})\}^m ,$$

$$ {}^{\text{n.d}}H_{\text{rot}} = \sum_m u_m^{(J)} \left[(J_+^2 + J_-^2), \{\mathbf{G}(\beta^{(J)})\}^m \right]_+ , \qquad (3)$$

$m = 0, 1, 2, 3 \ldots$; $J_\pm$ are the ladder operators of angular momentum; $[A, B]_+ = AB + BA$; **G** are simple non-polynomial functions of angular momentum:

$$\mathbf{G}(\alpha^{(J)}) = \frac{2}{\alpha^{(J)}} \left\{ \sqrt{1 + \alpha^{(J)} J_Z^2} - 1 \right\}. \qquad (4)$$

Formally, $\alpha^{(J)}$, $\beta^{(J)}$ and $g^{(J)}$, $u^{(J)}$ in Eqs. (3) and (4) are rotational operators:

$$\alpha^{(J)} = \sum_n \alpha_n J^{2n}; \quad g_m^{(J)} = \sum_n g_{nm} J^{2n}; \qquad (5)$$

$$\beta^{(J)} = \sum_n \beta_n J^{2n}; \quad u_m^{(J)} = \sum_n u_{nm} J^{2n}. \qquad (5a)$$

In this paper, we present only characteristic features of the model; a more detailed description can be found in Ref. 16. The interaction operators of the Fermi and Coriolis type were written in the following form:

$$H_F^{VV'} = F_0 + F_J^{VV'} J^2 + F_K^{VV'} J_Z^2 + F_{XY}^{VV'} (J_+^2 + J_-^2) + F_{JZ}^{VV'} J^2 J_Z^2, \qquad (6)$$

$$H_C^{VV'} = C_0^{VV'} (J_+ - J_-) + C_1^{VV'} \{J_+ (J_Z + 1/2) + (J_Z + 1/2) J_-\} + C_2^{VV'} J^2 (J_+ - J_-) + C_3^{VV'} J^2 \{J_+ (J_Z + 1/2) + (J_Z + 1/2) J_-\} + C_4^{VV'} J^4 (J_+ - J_-) \, C_5^{VV'} \{J_+^3 (J_Z + 3/2)^2 - (J_Z + 3/2) J_-^3\}. \qquad (6a)$$

Operator of the effective dipole moment

To calculate the line intensities in the bands $(\nu_1\ \nu_2\ \nu_3) \rightarrow (\nu_1'\ \nu_2'\ \nu_3')$, we used the formalism of the effective dipole moment operator, which significantly simplifies the procedure of calculation of transition probabilities by replacing calculation of matrix elements of the molecular dipole moment with respect to exact wave functions

$$\langle \Psi_a | \mu_Z | \Psi_b \rangle = {}^{\text{eff}}\langle \Psi_a | \tilde{\mu}_Z | \Psi_b \rangle^{\text{eff}} \qquad (7)$$

with calculation of matrix elements from the transformed dipole moment with respect to effective wave functions

$$|\Psi\rangle^{\text{eff}} = |\nu_1\ \nu_2\ \nu_3\ JK_aK_c\rangle^{\text{eff}} = \sum_{\text{v}\in\{P\}} |\mathbf{V}\rangle \sum_K C_{JK\gamma}^V |JK\gamma\rangle,$$

where V takes all values in the given polyad P; $|\mathbf{V}\rangle \equiv |\nu_1\rangle\,|\nu_2\rangle\,|\nu_3\rangle$ are harmonic oscillator wave functions; $|JK\gamma\rangle$ are symmetrized rotational wave functions, and the eigenvectors $C_{JK\gamma}^V$ are determined from diagonalization of the effective Hamiltonian matrix, i.e., in processing of line positions or energy levels.

The effective operator of dipole moment[12] can be represented in the form

$$\tilde{\mu}_Z = \sum_{VV'} |\mathrm{V}\rangle\, {}^{VV'}\tilde{\mu}_Z\, \langle \mathrm{V}'|, \qquad (8)$$

where ${}^{VV'}\tilde{\mu}_Z = \langle \mathbf{V}|\tilde{\mu}_Z|\mathbf{V}'\rangle$ is the so-called transformed transition moment. This procedure determines the transformed operators of transition moments as purely

rotational operators depending on the directional cosines φ_α and components of the operator of angular momentum J_α. The operator ${}^{VV'}\tilde{\mu}_Z$ is expanded into a series over the rotational operators

$$ {}^{VV'}\tilde{\mu}_Z = \sum_j {}^{VV'}\mu_j A_j, \qquad (8a)$$

where j numbers the elementary rotational operators. The standard determination of the rotational operators A_j for the bands of the A and B type up to $j = 8$ is given in Ref. 20. In this case, calculation of the line strengths of rotational-vibrational transitions

$$ S_{ab} = \left| \sum_{VV'KK'} \sum C^V_{JK\gamma} C^{V'}_{J'K'\gamma'} \sum_j {}^{VV'}\mu_j \langle JK\gamma | A_j | J'K'\gamma' \rangle \right|^2 \qquad (9)$$

depends on the knowledge of the coefficients $C^V_{JK\gamma}$ determined from diagonalization of the effective Hamiltonian matrix (1) and the coefficients ${}^{VV'}\tilde{\mu}_j$ considered as empiric parameters, whose values are found from solution of the inverse problem on line intensities.

Calculation of line parameters and discussion

For calculation of line positions, we used the Hamiltonian parameters given in Tables 1 and 2. These parameters were determined from processing of experimental energy levels of the first[21] and the second[22] triads.

Table 1. Spectroscopic constants for the first triad of interacting states of the water molecule, cm $^{-1}$

State 001		State 020		State 100	
Diagonal part					
Parameter	Value	Parameter	Value	Parameter	Value
$A_0 \cdot 10^{-2}$	0.744 ± 0.013	$A_0 \cdot 10^{-2}$	2.67 ± 0.10	$A_0 \cdot 10^{-2}$	0.921 ± 0.025
G_{00}	3755.933 ± 0.002	$A_1 \cdot 10^{-4}$	−0.16 ± 0.06	G_{00}	3654.1552 ± 0.0018
G_{10}	11.7831 ± 0.0001	G_{00}	3154.5310 ± 0.0002	G_{10}	11.6973 ± 0.0003
$G_{20} \cdot 10^{-2}$	−0.1289 ± 0.0003	G_{10}	11.9151 ± 0.0003	$G_{20} \cdot 10^{-2}$	−0.1241 ± 0.0003
$G_{30} \cdot 10^{-6}$	0.55 ± 0.02	$G_{20} \cdot 10^{-2}$	−0.159 ± 0.001	$G_{30} \cdot 10^{-6}$	0.51 ± 0.02
G_{01}	14.8660 ± 0.0004	$G_{30} \cdot 10^{-5}$	0.159 ± 0.016	G_{01}	15.4336 ± 0.0005
$G_{11} \cdot 10^{-2}$	0.578 ± 0.001	$G_{40} \cdot 10^{-8}$	−0.44 ± 0.07	$G_{11} \cdot 10^{-2}$	0.5514 ± 0.0012
$G_{21} \cdot 10^{-5}$	−0.22 ± 0.02	G_{01}	23.671 ± 0.001	$G_{21} \cdot 10^{-5}$	−0.207 ± 0.025
$G_{02} \cdot 10^{-2}$	−0.13 ± 0.04	$G_{11} \cdot 10^{-2}$	1.125 ± 0.004	$G_{02} \cdot 10^{-2}$	0.49 ± 0.09
$G_{12} \cdot 10^{-5}$	−0.41 ± 007	$G_{31} \cdot 10^{-6}$	0.109 ± 0.004	$G_{12} \cdot 10^{-5}$	−0.38 ± 0.09
$G_{03} \cdot 10^{-5}$	−0.87 ± 0.16	$G_{02} \cdot 10^{-2}$	4.49 ± 0.60	$G_{03} \cdot 10^{-4}$	−0.23 ± 0.06
		$G_{12} \cdot 10^{-3}$	−0.15 ± 0.03		
		$G_{22} \cdot 10^{-6}$	−0.92 ± 0.06		
		$G_{03} \cdot 10^{-3}$	−0.14 ± 0.05		
		$G_{13} \cdot 10^{-5}$	0.309 ± 0.030		
		$G_{04} \cdot 10^{-5}$	−0.219 ± 0.038		
Off-diagonal part					
$B_0 \cdot 10^{-1}$	0.10 ± 0.01	$B_0 \cdot 10^{-1}$	0.55 ± 0.06	$B_0 \cdot 10^{-1}$	0.141 ± 0.018
U_{00}	1.3229 ± 0.0001	U_{00}	1.4652 ± 0.0001	U_{00}	1.3007 ± 0.0001
$U_{10} \cdot 10^{-3}$	−0.527 ± 0.002	$U_{10} \cdot 10^{-3}$	−0.663 ± 0.003	$U_{10} \cdot 10^{-3}$	−0.501 ± 0.002
$U_{20} \cdot 10^{-6}$	0.27 ± 0.07	$U_{20} \cdot 10^{-6}$	0.494 ± 0.025	$U_{20} \cdot 10^{-6}$	0.244 ± 0.018
$U_{01} \cdot 10^{-2}$	−0.123 ± 0.001	$U_{01} \cdot 10^{-2}$	−0.909 ± 0.007	$U_{01} \cdot 10^{-2}$	−0.128 ± 0.001
$U_{02} \cdot 10^{-4}$	0.205 ± 0.008	$U_{21} \cdot 10^{-7}$	−0.534 ± 0.044	$U_{02} \cdot 10^{-4}$	0.226 ± 0.009
		$U_{02} \cdot 10^{-3}$	0.251 ± 0.011		
		$U_{12} \cdot 10^{-6}$	0.881 ± 0.072		
		$U_{03} \cdot 10^{-5}$	−0.419 ± 0.044		
Resonance parameters					
Fermi resonance between the states 100–020		Coriolis resonance between the states 020–001		Coriolis resonance between the states 100–001	
F_0	38.15	C_0	0.808 ± 0.042	C_0	−0.147 ± 0.009
F_J	0.0282 ± 0.0016	C_1	0.113 ± 0.002	C_1	0.308 ± 0.001
F_K	−0.144 ± 0.001				
F_{xy}	−0.0070 ± 0.0003				

Table 2. Spectroscopic constants for the second triad of interacting states of the water molecule, cm $^{-1}$

State 110		State 030		State 011	
Diagonal part					
Parameter	Value	Parameter	Value	Parameter	Value
$A_0 \cdot 10^{-2}$	5.27 ± 3.40	$A_0 \cdot 10^{-2}$	6.55 ± 1.40	$A_0 \cdot 10^{-2}$	1.59 ± 0.07
$A_1 \cdot 10^{-4}$	1.69 ± 0.55	$A_1 \cdot 10^{-4}$	−2.49 ± 0.24	$A_1 \cdot 10^{-4}$	1.603 ± 0.003
G_{00}	5229.026 ± 0.002	$A_3 \cdot 10^{-8}$	0.25 ± 0.08	G_{00}	5331.268 ± 0.002
G_{10}	11.738 ± 0.001	G_{00}	4672.740 ± 0.002	G_{10}	11.8013 ± 0.0002
$G_{20} \cdot 10^{-2}$	−0.141 ± 0.001	G_{10}	11.878 ± 0.001	$G_{20} \cdot 10^{-2}$	−0.1450 ± 0.0003
$G_{30} \cdot 10^{-6}$	0.71 ± 0.11	$G_{20} \cdot 10^{-2}$	−0.174 ± 0.001	$G_{30} \cdot 10^{-6}$	0.66 ± 0.01
$G_{40} \cdot 10^{-9}$	−0.36 ± 0.30	$G_{30} \cdot 10^{-5}$	0.115 ± 0.016	G_{01}	17.7300 ± 0.0008
G_{01}	18.467 ± 0.002	G_{01}	30.223 ± 0.003	$G_{11} \cdot 10^{-2}$	0.769 ± 0.002
$G_{11} \cdot 10^{-2}$	0.75 ± 0.01	$G_{11} \cdot 10^{-2}$	1.55 ± 0.02	$G_{21} \cdot 10^{-5}$	0.266 ± 0.019
$G_{21} \cdot 10^{-5}$	0.24 ± 0.12	$G_{21} \cdot 10^{-4}$	0.53 ± 0.05	$G_{02} \cdot 10^{-2}$	2.05 ± 0.30
$G_{31} \cdot 10^{-8}$	0.73 ± 0.53	G_{02}	0.24 ± 0.11	$G_{12} \cdot 10^{-3}$	0.683 ± 0.001
G_{02}	0.189 ± 0.11	$G_{12} \cdot 10^{-3}$	−2.02 ± 0.18	$G_{03} \cdot 10^{-4}$	−0.91 ± 0.13
$G_{12} \cdot 10^{-3}$	0.82 ± 0.25	$G_{22} \cdot 10^{-6}$	−2.48 ± 1.06		
$G_{03} \cdot 10^{-2}$	−0.104 ± 0.090	$G_{32} \cdot 10^{-7}$	0.17 ± 0.08		
$G_{22} \cdot 10^{-6}$	−0.128 ± 0.050	$G_{03} \cdot 10^{-3}$	−2.04 ± 1.05		
$G_{13} \cdot 10^{-5}$	−0.419 ± 0.220	$G_{13} \cdot 10^{-5}$	2.69 ± 0.30		
$G_{04} \cdot 10^{-6}$	0.469 ± 0.219	$G_{23} \cdot 10^{-7}$	−0.32 ± 0.14		
Off-diagonal part					
$B_0 \cdot 10^{-1}$	1.25 ± 0.01	$B_0 \cdot 10^{-1}$	0.94 ± 0.11	$B_0 \cdot 10^{-1}$	5.76 ± 0.03
U_{00}	1.3833 ± 0.0002	$B_1 \cdot 10^{-3}$	−0.37 ± 0.08	U_{00}	1.4057 ± 0.0001
$U_{10} \cdot 10^{-3}$	−0.571 ± 0.007	$B_2 \cdot 10^{-6}$	0.86 ± 0.20	$U_{10} \cdot 10^{-3}$	−0.598 ± 0.002
$U_{20} \cdot 10^{-6}$	0.34 ± 0.06	U_{00}	1.5416 ± 0.0003	$U_{20} \cdot 10^{-6}$	0.373 ± 0.007
$U_{01} \cdot 10^{-2}$	−0.381 ± 0.016	$U_{10} \cdot 10^{-3}$	−0.763 ± 0.010	$U_{01} \cdot 10^{-2}$	−0.342 ± 0.002
$U_{11} \cdot 10^{-5}$	−0.43 ± 0.15	$U_{20} \cdot 10^{-6}$	0.575 ± 0.095	$U_{02} \cdot 10^{-4}$	0.726 ± 0.014
$U_{12} \cdot 10^{-6}$	0.27 ± 0.13	$U_{01} \cdot 10^{-2}$	−2.658 ± 0.067	$U_{11} \cdot 10^{-5}$	−0.36 ± 0.01
		$U_{11} \cdot 10^{-4}$	0.11 ± 0.04		
		$U_{02} \cdot 10^{-3}$	1.78 ± 0.09		
		$U_{12} \cdot 10^{-6}$	−1.13 ± 0.41		
		$U_{03} \cdot 10^{-4}$	−0.41 ± 0.03		
		$U_{04} \cdot 10^{-6}$	0.25 ± 0.03		

Resonance parameters					
Fermi resonance between the states 110–030		Coriolis resonance between the states 011–030		Coriolis resonance between the states 011–110	
F_0	57.83115	C_0	−0.84 ± 0.03	C_1	−0.299 ± 0.001
F_J	−0.121 ± 0.005	$C_2 \cdot 10^{-3}$	−0.49 ± 0.40	C_3	0.308 ± 0.001
F_K	−0.179 ± 0.001	$C_3 \cdot 10^{-3}$	0.411 ± 0.024	$C_4 \cdot 10^{-5}$	0.102 ± 0.018
$F_{xy} \cdot 10^{-1}$	−0.117 ± 0.002	$C_4 \cdot 10^{-5}$	−0.61 ± 0.14	$C_5 \cdot 10^{-4}$	−0.452 ± 0.033
$F_{JZ} \cdot 10^{-2}$	0.177 ± 0.006	$C_5 \cdot 10^{-4}$	0.149 ± 0.015		

For the first triad, 363 energy levels up to the rotational quantum number $J = 10$ were selected and the set of 66 parameters was determined. These parameters reconstruct the experimental levels with the accuracy of 0.0045 cm^{-1}. For the second triad of interacting states, 578 energy levels up to the rotational quantum number $J = 14$ were selected, and the set of 85 spectroscopic parameters was determined, which reconstructs the experimental levels with the accuracy of 0.011 cm^{-1}.

The determined spectroscopic constants allowed us to calculate line positions for the set of hot bands {030, 110, 011–001, 020, 100}. To calculate line intensities of hot transitions {030–020, 110–100, 011–001}, the coefficients $^{VV'}\tilde{\mu}_j$ were re-calculated based on the known empiric parameters for cold transitions.[23,24] The main contributions to the transformed transition moment for the bands {110–001, 011–100, 011–020} were determined from the obtained values of the second $^{z}\mu_{23}$ and third $^{z}\mu_{123}$ derivatives of the dipole moment function of the water molecule[15]; the corresponding values are given in Table 3.

There is a peculiarity in calculating of the parameters of the transformed transition moment of the band {110–020} that should be noted. It is well-known that the value of the second derivative of the

dipole moment function ${}^{x}\mu_{12} = -(8.43 \pm 1.8) \cdot 10^{-3}$ D determined from the empiric parameters of the band {110–000} does not allow the probability of the hot band {100–010} to be reconstructed with the experimental accuracy.[25,26] Calculation with this value underestimates the intensities in the band {100–010}. Therefore, to determine line intensities of the hot band {110–020}, we used the re-calculated semiempirical parameters of the transition moment of the band {100–010} from Ref. 26. Table 3 presents the parameters of transition moments, which were used in our calculations.

Table 4 and Fig. 2 summarize calculated results on the line parameters for the hot bands forming the 6.3-μm band. Table 4 presents the frequency intervals, the number of lines in this interval, the maximum intensity in a band, and the integral intensity. The integral intensities of the bands were determined by means of direct summation of intensities of all lines starting from $1.0 \cdot 10^{-30}$ ($\text{cm}^{-1}/(\text{mol} \cdot \text{cm}^{-2})$ at $T = 296$ K). This restriction is well justified taking into account the part of weak absorption lines. Table 4 also compares our results with the results of Ref. 9, in which line intensities were calculated based on *ab initio* calculations of the dipole moment function of the water molecule. One can see quite good agreement between the results. Some differences can be adequately explained. For the band 030–020, as was noted in Ref. 9, the obtained value of the integral intensity exceeded the experimental value by 25%, and it exceeds our value just by 25% too. Unfortunately, experimental data for other bands are absent, and it is still impossible to say which calculation is more accurate.

Table 3. Parameters of vibrational transition moments $\mu_j^{VV'}$ used in our calculations, D (debye)

Parameter	Transition 030–020	Transition 110–100	Transition 011–001
μ_1	0.22289	0.129	0.129
μ_2	$1.997 \cdot 10^{-5}$	$0.115 \cdot 10^{-4}$	$0.115 \cdot 10^{-4}$
μ_3	$1.00547 \cdot 10^{-4}$	$0.58 \cdot 10^{-4}$	$0.58 \cdot 10^{-4}$
μ_4	−0.01132	$-0.65 \cdot 10^{-2}$	$-6.5 \cdot 10^{-3}$
μ_5	$-3.96183 \cdot 10^{-4}$	$-0.229 \cdot 10^{-3}$	$-0.229 \cdot 10^{-3}$
μ_6	$-3.34867 \cdot 10^{-5}$	$-0.19 \cdot 10^{-4}$	$-0.19 \cdot 10^{-4}$
μ_7	$1.34642 \cdot 10^{-4}$	$0.777 \cdot 10^{-4}$	$0.777 \cdot 10^{-4}$
μ_8	$-1.54459 \cdot 10^{-5}$	$-0.89 \cdot 10^{-5}$	$-0.89 \cdot 10^{-5}$
	Transition 110–001	Transition 011–100	Transition 030–001
μ_1	$6.9 \cdot 10^{-3}$	$8.1 \cdot 10^{-3}$	0.0
	Transition 110–020	Transition 011–020	Transition 030–100
μ_1	0.0283	0.0354	0.0

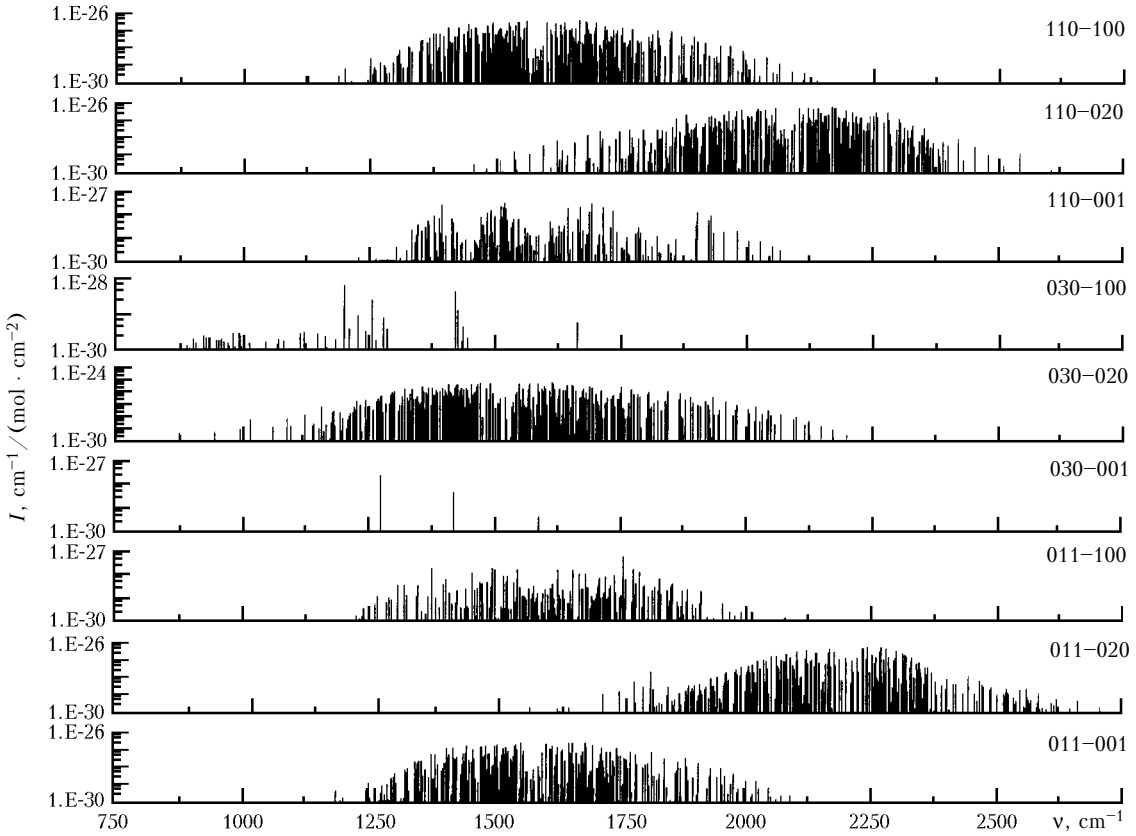

Fig. 2. General view of the absorption spectra of hot bands. Intensities are given in the logarithmic scale.

Table 4. Parameters of vibrational bands of the water molecule in the region of 6.3 μm

Transition	Region, cm^{-1}	Number of lines	$I_{max} \cdot 10^{24}$ $cm^{-1}/(mol \cdot cm^{-2})$ at T = 296 K	Integral intensity $S \cdot 10^{24}$ $cm^{-1}/(mol \cdot cm^{-2})$ at T = 296 K	
				Our result	Ref. 9
030–001	1238–1588	4	$0.2910 \cdot 10^{-3}$	$0.3500 \cdot 10^{-3}$	$0.3476 \cdot 10^{-3}$
030–020	872–2221	542	$0.1710 \cdot 10^{-2}$	5.678	7.113
030–100	889–1661	73	$0.7170 \cdot 10^{-4}$	$0.3388 \cdot 10^{-3}$	$0.1286 \cdot 10^{-2}$
110–001	1226–2127	255	$0.3970 \cdot 10^{-3}$	$0.6834 \cdot 10^{-2}$	$0.7985 \cdot 10^{-2}$
110–020	1454–2603	451	$0.8120 \cdot 10^{-2}$	0.2819	0.1261
110–100	1125–2137	472	$0.5810 \cdot 10^{-2}$	0.2061	0.2194
011–001	1133–2114	454	$0.3310 \cdot 10^{-2}$	0.1197	0.1263
011–020	1483–2712	452	$0.9170 \cdot 10^{-2}$	0.2221	0.2243
011–100	1208–2251	310	$0.8390 \cdot 10^{-3}$	$0.7866 \cdot 10^{-2}$	$0.7009 \cdot 10^{-2}$

It should be emphasized that the known HITRAN and GEISA databases do not include such calculations. The performed analysis of experimental data on line intensities of the water molecule calls for improving the qualitative description of intensities.[26,27] Modernization of the models used for processing of intensities will allow the parameters of the dipole moment function of the water molecule to be determined with higher accuracy, what, in its turn, will improve the direct calculations of the intensities of hot bands.

Acknowledgments

The authors are thankful to S.N. Mikhailenko for useful discussions and recommendations and S.A. Tashkun for the possibility of using the GIP program.

This work was partly supported by Russian Foundation for Basic Research Grant No. 00–05–65082 and CNRS–RFBR PICS Grant No. 01–05–22002.

References

1. G.S. Golisyn, A.I. Semenov, N.N. Shefov, L.M. Fishkova, and S.P. Perov, Geophys. Res. Lett. **23**, No. 14, 1741–1744 (1996).
2. A.I. Semenov, Geomagnitizm i Aeron. **37**, No. 3, 132–142 (1997).
3. G. Zaragoza, M. Lopez-Puertas, A. Lambert, J.J. Remedios, and F.W. Taylor, J. Geophys. Res. D **103**, No. 23, 31293–31308 (1998).
4. D.K. Zhou, M.G. Mlynczak, M. Lopez-Puertas, and G. Zaragoza, Geophys. Res. Lett. **26**, No. 1, 67–70 (1999).
5. M. Lopez-Puertas, G. Zaragoza, M.A. Lopez-Valverde, F.J. Martin-Torres, G.M. Shved, R.O. Manuilova, A.A. Kutepov, O.A. Gusev, T. Von Clarmann, G. Stiller, A. Wegner, H. Oelhaf, D.P. Edwards, and J.-M. Flaud, J. Quant. Spectrosc. Radiat. Transfer **59**, Nos. 3–5, 377–403 (1998).
6. R.O. Manuilova and G.M. Shved, J. Atmos. Terr. Phys. **47**, No. 5, 413–422 (1985).
7. M. Lopez-Puertas, G. Zaragoza, B.J. Kerridge, and F.W. Taylor, J. Geophys. Res. D **100**, No. 5, 9131–9147 (1995).
8. H. Partridge and D.W. Schwenke, J. Chem. Phys. **106**, No. 11, 4618–4639 (1997).
9. H. Partridge and D.W. Schwenke, J. Chem. Phys. **113**, No. 16, 6592–6597 (2000).
10. Yu.S. Makushkin and Vl.G. Tyuterev, *Perturbation Methods and Effective Hamiltonians* (Nauka, Novosibirsk, 1984), 236 pp.
11. M.R. Aliev and J.K.G. Watson, in: *Molecular Spectroscopy: Modern Research* (Academic Press, 1985), Vol. 3, pp. 1–69.
12. C. Camy-Peyret and J.M. Flaud, in *Molecular Spectroscopy: Modern Research* (Academic Press, 1985), Vol. 3, pp. 70–117.
13. O.N. Sulakshina, Yu.G. Borkov, Vl.G. Tyuterev, and A. Barbe, J. Chem. Phys. **113**, No. 23, 10572–10582 (2000).
14. O.N. Sulakshina and Yu. Borkov, in: *The 15th International Conference on High Resolution Molecular Spectroscopy. Programme and Abstracts* (Prague, 1998), p. 180.
15. O.N. Sulakshina, Yu. Borkov, A. Barbe, and Vl.G. Tyuterev, in: *IRS2000: Current Problems in Atmospheric Radiation* (A. Deepak Publishing, 2001), Vol. 147, pp. 651–655.
16. A.D. Bykov, L.N. Sinitsa, and V.I. Starikov, *Experimental and Theoretical Methods in Spectroscopy of Water Vapor Molecules* (SB RAS Publishing House, Novosibirsk, 1999), 376 pp.
17. Vl.G. Tyuterev, V.I. Starikov, S.A. Tashkun, and S.N. Mikhailenko, J. Mol. Spectrosc. **170**, No. 1, 38–58 (1995).
18. V.I. Starikov and S.N. Mikhailenko, J. Mol. Struct. **442**, 39–53 (1998).
19. V.I. Starikov and S.N. Mikhailenko, J. Mol. Struct. **449**, 39–51 (1998).
20. C. Camy-Peyret and J.M. Flaud, *These de Doctorat es Sciences* (Universite Pierre et Marie Curie, Paris, 1975).
21. S.N. Mikhailenko, Vl.G. Tyuterev, K.A. Keppler, B.P. Winnewisser, M. Winnewisser, G. Mellau, S. Klee, and K.N. Rao, J. Mol. Spectrosc. **184**, No. 3, 330–349 (1997).
22. S.N. Mikhailenko, Vl.G. Tyuterev, V.I. Starikov, K.K. Albert, B.P. Winnewisser, M. Winnewisser, G. Mellau, C. Camy-Peyret, R. Lanquetin, J.M. Flaud, and J.W. Brault, J. Mol. Spectrosc. (in press).
23. J.M. Flaud and C. Camy-Peyret, J. Mol. Spectrosc. **55**, No. 2, 278–310 (1975).
24. C. Camy-Peyret and J.M. Flaud, Mol. Phys. **32**, No. 2, 523–537 (1976).
25. J.M. Flaud, C. Camy-Peyret, J.-Y. Mandin, and G. Guelachvili, Mol. Phys. **34**, No. 2, 413–426 (1977).
26. R. Toth, J. Opt. Soc. Am. B **10**, No. 11, 2006–2029 (1993).
27. R. Toth, J. Mol. Spectrosc. **194**, 28–42 (1999).